Journal of Information Systems Engineering and Management
2024, 9(4)
e-ISSN: 2468-4376
https://www.jisem-journal.com/

Research Article

First-Principles Study of Half-Metallicity and Optical Properties in Co2CrX (X = Al, Bi, Ge, Si) Heusler Compounds

Malsawmtluanga[1], Lalrintluanga Sailo[2*], Zaithanzauva Pachuau[3], Lawrence Zonunmawia[4], Lalmuanawma[5], Lalnunpuia[6]
[1]Research Scholar, Mizoram University, Aizawl, Mizoram, India
[2,4]Department of Physics, Govt. Zirtiri Res. Sc. College, Aizawl, Mizoram, India
[3]Department of Physics, Mizoram University, Aizawl, Mizoram, India
[5]Department of Physics, Lunglei Govt. College, Lunglei, Mizoram, India
[6]Department of Physics, Govt. Champhai College, Champhai, Mizoram, India
[*]Corresponding Author: lalrinasailo@gmail.com

ARTICLE INFO

Received: 02 Sept 2024

Accepted: 19 Oct 2024

Published: 28 Oct 2024

ABSTRACT

In this work, we present a systematic first-principles investigation of the structural, electronic, magnetic, elastic, and optical properties of Co2CrX (X = Al, Bi, Ge, Si) full-Heusler compounds. The calculations are performed using the full-potential linearized augmented plane wave (FP-LAPW) method as implemented in the WIEN2k code within the framework of the generalized gradient approximation (GGA). Our results indicate that all studied compounds crystallize in the cubic L21 structure and exhibit half-metallic ferromagnetism with nearly 100% spin polarization, highlighting their strong potential for spintronic applications. Analysis of the electronic band structure and density of states reveals the presence of a band gap in the minority-spin channel, while the majority-spin states remain metallic at the Fermi level. The calculated total magnetic moments follow the Slater-Pauling rule and are predominantly contributed by Co and Cr atoms. Furthermore, optical properties including the dielectric function, reflectivity, absorption coefficient, optical conductivity, refractive index, and electron energy loss function are evaluated within the interband transition regime. The optical response demonstrates pronounced light–matter interaction and significant dispersion characteristics, suggesting suitability for optoelectronic applications.

Keywords: Heusler compounds, First-principles calculations, Half-metallicity, Spintronics, Optical properties.

1. Introduction

Heusler compounds have attracted considerable scientific interest since their discovery in 1903, when German chemist Friedrich Heusler reported that the intermetallic compound Cu_2MnAl exhibits ferromagnetism despite being composed of non-magnetic elements [1]. This remarkable finding challenged existing theories of magnetism and laid the foundation for extensive research into this class of materials.

Subsequent studies in the early 20th century identified additional ferromagnetic Heusler alloys, including Cu_2MnSn, Cu_2MnSb, and Cu_2MnBi, all of which crystallize in the cubic $L2_1$ structure. The ordered $L2_1$ phase, consisting of four interpenetrating face-centered cubic (fcc) sublattices, was systematically characterized by Bradley and Rogers in the 1930s, providing detailed insight into atomic site occupation [2].

Journal of Information Systems Engineering and Management
2024, 9(4)
e-ISSN: 2468-4376
https://www.jisem-journal.com/

Research Article

A major breakthrough occurred in 1983 when Robert A. de Groot and co-workers predicted half-metallic ferromagnetism in the semi-Heusler compound NiMnSb [3]. In such materials, one spin channel exhibits metallic behavior while the other displays a band gap, resulting in 100% spin polarization at the Fermi level, an essential feature for spintronic applications.

At present, the Heusler family encompasses thousands of compounds, including full-, half-, inverse-, and quaternary Heuslers, which exhibit diverse magnetic and electronic properties. These materials are of significant interest due to their tunable band structures and potential applications in spintronics, thermoelectrics, and topological materials [4].

Among them, full-Heusler alloys with the general formula A_2BX (where A and B are transition metals and X is a main-group element) crystallize in the cubic $L2_1$ structure with a 2:1:1 stoichiometry [5–7]. These compounds exhibit a wide range of physical properties, making them attractive candidates for multifunctional applications.

In the present work, we perform a detailed first-principles study of Co_2CrX (X = Al, Bi, Ge, Si) full-Heusler compounds. The calculations are conducted within the framework of density functional theory using the GGA approach as implemented in WIEN2k [8]. We systematically investigate their structural, electronic, magnetic, elastic, and optical properties to assess their suitability for advanced spintronic and optoelectronic applications.

2. Computational Methodology

The structural, electronic, optical, and magnetic properties of the Co_2CrX (X = Al, Bi, Ge, Si) full-Heusler compounds were investigated using the full-potential linearized augmented plane wave (FP-LAPW) method [9], as implemented in the WIEN2k package. The exchange-correlation effects were treated within the generalized gradient approximation (GGA) using the Perdew–Burke–Ernzerhof (PBE) functional [10]. Spin-orbit coupling (SOC) was included in all calculations to account for relativistic effects, which are particularly significant for heavier elements such as Bi.

Within the WIEN2k formalism, the core states were treated fully relativistically, while the valence states were described using a semi-relativistic approximation. The energy cutoff separating core and valence states was set to −6.0 Ry. Brillouin zone integrations were performed using a Monkhorst–Pack k-point mesh comprising 1000 k-points for self-consistent field (SCF) calculations. For optical property calculations, a denser k-point grid of 10,000 points was employed to ensure improved numerical precision.

The basis set size was controlled by the parameter $R_{MT}\times K_{max}$, which was chosen to be 7.0, where R_{MT} represents the muffin-tin radius and K_{max} denotes the maximum magnitude of the reciprocal lattice vector. The self-consistency cycle was considered converged when the total energy difference between successive iterations was less than 0.0001 Ry. The wave functions inside the atomic spheres were expanded up to a maximum angular momentum quantum number of l_{max} =10. In the interstitial region, the charge density and potential were expanded in a Fourier series with a cutoff parameter of G_{max} =10.

The muffin-tin radii (R_{MT}) for all atomic species were carefully selected to avoid sphere overlap while ensuring optimal representation of the basis functions. The corresponding values are listed in Table 1.

Table 1: Muffin tin radius (R_{MT}) for Co_2CrX (X = Al, Bi, Ge, Si)

Compound	R_{MT} (a.u)		
	Co	Cr	X
Co_2CrAl	2.37	2.27	2.16
Co_2CrBi	2.14	2.13	2.26
Co_2CrGe	2.22	2.11	2.12
Co_2CrSi	2.26	2.16	1.90

Journal of Information Systems Engineering and Management
2024, 9(4)
e-ISSN: 2468-4376
https://www.jisem-journal.com/

Research Article

To investigate the magnetic and spin-resolved electronic properties, both spin-up and spin-down channels were explicitly considered for all atomic species. A 10×10×10 Monkhorst–Pack *k*-point mesh was used for Brillouin zone sampling [11], ensuring a good compromise between computational efficiency and accuracy in total energy and magnetic moment calculations. During structural optimization, all atomic positions were relaxed without constraints in the *x*-, *y*-, and *z*-directions, allowing the system to reach its ground state geometry with minimal forces and stress.

3. Crystal Structure

The investigated Co_2CrX (X = Al, Bi, Ge, Si) full-Heusler compounds crystallize in the cubic $L2_1$ structure with space group Fm-3m (No. 225). The general formula of full-Heusler alloys is A_2BX, reflecting a 2:1:1 stoichiometry, where A and B are typically transition metals (d-block elements), and X is a main-group element (p-block metal or semimetal) [12,13].

The $L2_1$ crystal structure consists of four interpenetrating face-centered cubic (fcc) sublattices. In the conventional unit cell, the atomic positions are given as: A_1 at (¼, ¼, ¼), A_2 at (¾, ¾, ¾), B at (0, 0, 0), and X at (½, ½, ½). This highly symmetric atomic arrangement plays a crucial role in determining the electronic, magnetic, and mechanical properties of the compounds.

To determine the equilibrium structural parameters, volume optimization was performed by fitting the calculated total energy as a function of volume to the Murnaghan equation of state [14]. This equation establishes the relationship between total energy E and volume V as follows:

$$E(V) = E_0 + \frac{B_0 V}{B_0'(B_0'-1)}\left[\left(\frac{V_0}{V}\right)^{B_0'-1} + 1\right] - \frac{B_0 V_0}{B_0' - 1}$$

where E_0 is the minimum energy at T = 0 K, V_0 is the equilibrium volume, B_0 is the bulk modulus, B_0' is the pressure derivative of the bulk modulus.

The results of the structural optimization are shown in Figure 1. The calculated values of the optimized lattice parameters, minimum energy, bulk modulus, and its pressure derivative are summarized in Table 2.

Table 2: Lattice Parameter, Bulk modulus, Equilibrium energy and Pressure derivative for Co_2CrX (X= Al, Bi, Ge, Si)

	Lattice Constants a_0 (Å)		Bulk modulus (GPa)		Equilibrium energy (E_0)	Pressure derivative
	Our Calc.	Others	Our Calc.	Others		
Co_2CrAl	5.710	5.73[15] 5.727[16]	196.671	195[23]	−8142.954	4.923
Co_2CrBi	5.649	5.65[17] 5.63[18]	396.351	406[24]	−50824.088	−0.944
Co_2CrGe	5.742	5.77[19] 5.74[20]	217.234	250.4[25]	−11856.872	4.132
Co_2CrSi	5.731	5.87[21] 5.87[22]	392.060	405.5[26]	−48241.791	0.143

Journal of Information Systems Engineering and Management
2024, 9(4)
e-ISSN: 2468-4376
https://www.jisem-journal.com/

Research Article

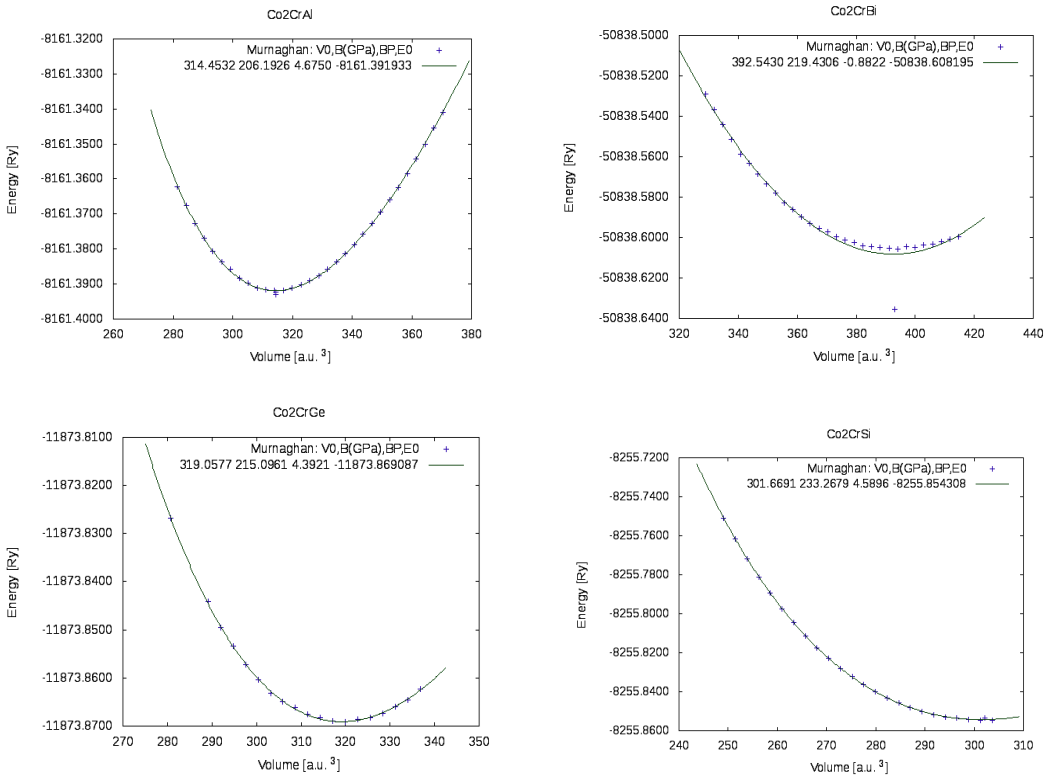

Fig. 1: Volume optimization curve for the lattice parameters

4. Electronic properties

Spintronics has emerged as a transformative paradigm in modern electronics, enabling devices that exploit not only the charge of electrons but also their intrinsic spin. This dual functionality offers significant advantages, including enhanced data processing speeds, reduced energy consumption, and lower heat dissipation. A key class of materials in this field is half-metallic ferromagnets, which exhibit 100% spin polarization at the Fermi level.

Full-Heusler alloys, particularly Co_2CrX (X = Al, Bi, Ge, Si), have attracted considerable attention due to their potential in spintronic applications. In the present study, spin-polarized calculations were performed within the generalized gradient approximation (GGA) at the optimized lattice parameters. The electronic structure analysis indicates that these compounds display metallic behavior in one spin channel, while the opposite spin channel exhibits a semiconducting gap, an essential characteristic of half-metallicity. The degree of spin polarization at the Fermi level is quantified using the following relation:

$$P_n = \frac{\rho\uparrow(E_F) - \rho\downarrow(E_F)}{\rho\uparrow(E_F) + \rho\downarrow(E_F)}$$

where $\rho\uparrow(E_F)$ and $\rho\downarrow(E_F)$ denote the densities of states at the Fermi level for spin-up and spin-down electrons, respectively. A value of $P_n = \pm 1$ corresponds to complete spin polarization, indicating that only one spin channel contributes to electrical conduction. Such behavior is highly desirable for applications in magnetic sensors, spin transistors, and non-volatile memory devices. Conversely, $P_n = 0$ signifies the absence of spin polarization, typical of paramagnetic or antiferromagnetic systems, even below the magnetic transition temperature [27].

Journal of Information Systems Engineering and Management
2024, 9(4)
e-ISSN: 2468-4376
https://www.jisem-journal.com/

Research Article

To further elucidate the electronic characteristics of Co_2CrX compounds, the density of states (DOS) and band structures were analyzed using the WIEN2k code. The results reveal the presence of a band gap in the minority-spin channel, with calculated values of 0.696 eV (Al), 0.258 eV (Bi), 0.603 eV (Ge), and 0.849 eV (Si). These findings confirm the half-metallic nature of the studied compounds and their associated 100% spin polarization.

A summary of the calculated band gaps and corresponding spin polarization values is provided in Table 3, while Figures 2 and 3 illustrate the detailed band structures and density of states.

Table 3: Energy gap and spin polarization of Co_2CrX (X= Al, Bi, Ge, Si) Compounds

	Energy gap Eg (eV)		Spin polarization
	Up spin	Down spin	
Co2CrAl	0.0	0.696	100%
Co2CrBi	0.0	0.258	100%
Co2CrGe	0.0	0.603	100%
Co2CrSi	0.0	0.849	100%

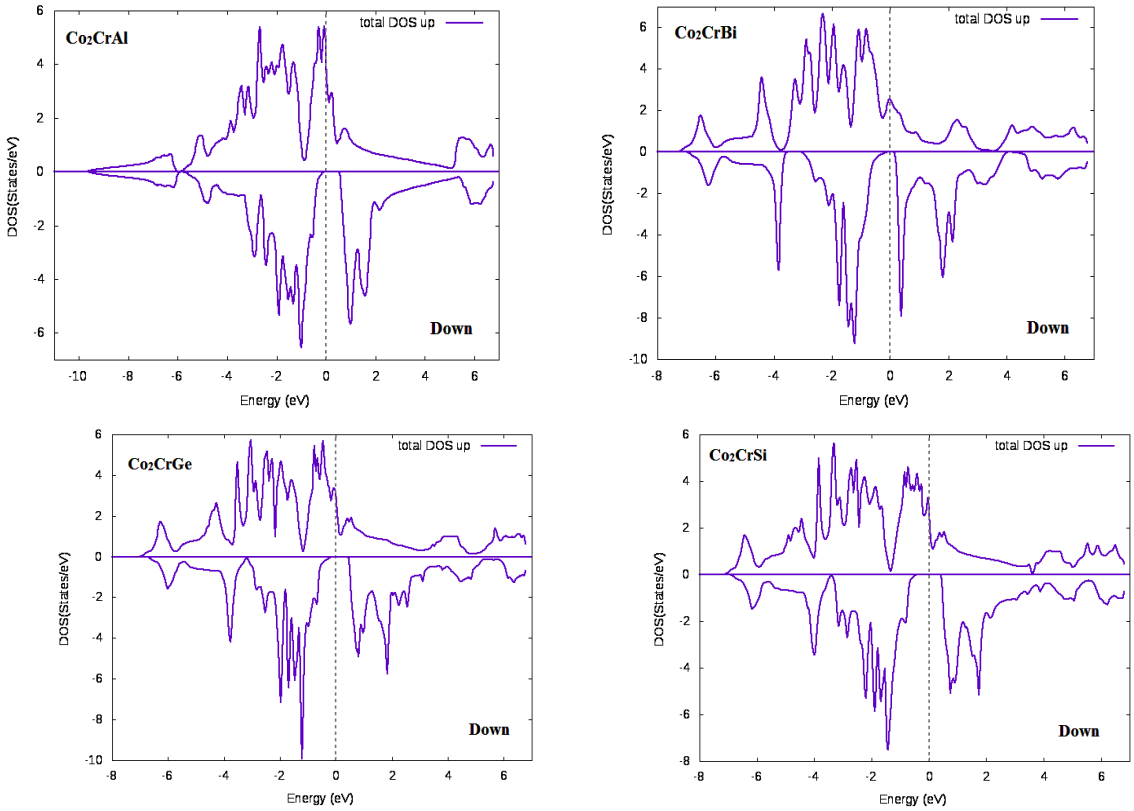

Fig. 2: DOS of Co_2CrX (X= Al, Bi, Ge, Si) using WIEN2k code

Journal of Information Systems Engineering and Management
2024, 9(4)
e-ISSN: 2468-4376
https://www.jisem-journal.com/

Research Article

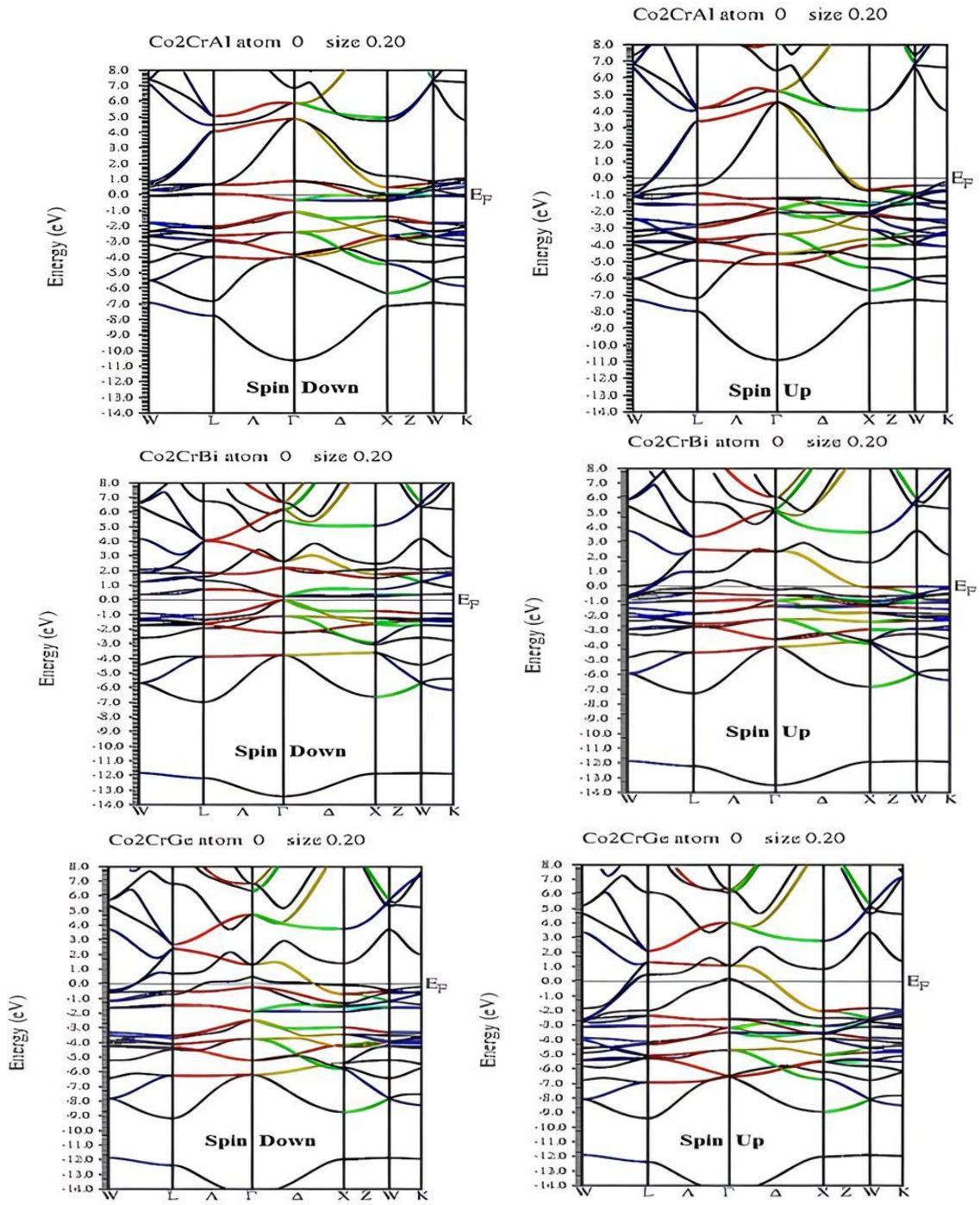

Journal of Information Systems Engineering and Management
2024, 9(4)
e-ISSN: 2468-4376
https://www.jisem-journal.com/

Research Article

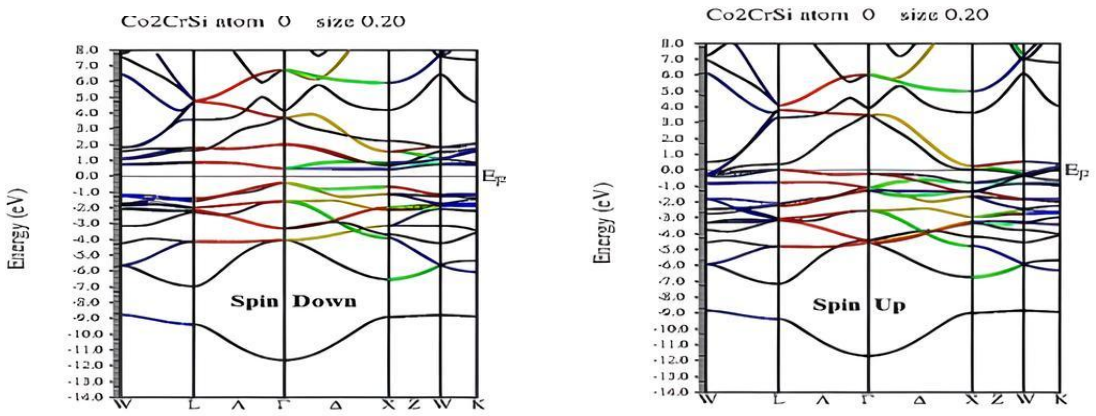

Fig. 3: Band Structure of Co_2CrX (X = Al, Bi, Ge, Si) using WIEN2k code

5. Magnetic properties

The magnetic behavior of Heusler alloys is strongly governed by their valence electron concentration (VEC). A critical threshold occurs at 24 valence electrons per formula unit, where compounds typically exhibit non-magnetic semiconducting behavior. For instance, Fe_2VAl, a well-known Heusler compound, possesses exactly 24 valence electrons and displays non-magnetic characteristics, with Fe atoms remaining in a non-magnetic state [27,28].

In contrast, Co_2BX-type Heusler alloys generally contain more than 24 valence electrons and exhibit ferromagnetic behavior that follows the Slater-Pauling rule. This empirical relationship connects the total number of valence electrons (Z_t) to the total magnetic moment (M) per formula unit:

$$M = Z_t - 24$$

In half-metallic ferromagnetic Heusler compounds, the Curie temperature is often found to increase approximately linearly with the valence electron count, with an estimated increment of about 175 K per additional valence electron. For example, Co_2CrAl, which has 27 valence electrons, exhibits a total magnetic moment of 3 μB per formula unit. This compound is ferromagnetic, with the magnetic moment primarily localized on the Co atoms, and shows a Curie temperature of approximately 525 K.

For the Co_2CrX (X = Al, Bi, Ge, Si) compounds investigated in this work, the calculated valence electron counts are 27, 29, 28, and 28, respectively. According to the Slater–Pauling rule, these correspond to total magnetic moments of 3.0, 5.0, 4.0, and 4.0 μB per formula unit. The computed results, obtained using the FP-LAPW method within the WIEN2k framework and the GGA approximation, show excellent agreement with these predictions. A summary of the calculated magnetic moments is presented in Table 4.

Further analysis indicates that the dominant contribution to the total magnetic moment arises from the Co and Cr atomic sites, while the X-site atoms contribute only marginally. Additionally, an increase in the valence electron count at the X-site enhances the magnetic moments at the Co and Cr sites, thereby strengthening the overall ferromagnetic behavior of the compounds.

Table 4: Total magnetic moments of the compounds Co_2CrX (X= Al, Bi, Ge, Si).

Compound	Zt	Magnetic moment (μ_B)	
		Calculated	Slater-Pauling
Co_2CrAl	27	3.01	3.00
Co_2CrBi	29	5.02	5.00

Journal of Information Systems Engineering and Management
2024, 9(4)
e-ISSN: 2468-4376
https://www.jisem-journal.com/

Research Article

Co_2CrGe	28	4.01	4.00
Co_2CrSi	28	4.01	4.00

6. Optical properties

Optical properties play a crucial role in determining the suitability of materials for optoelectronic applications. In this section, we analyze the optical response of Co_2CrX (X = Al, Bi, Ge, Si) full-Heusler compounds through key parameters, including the dielectric function, optical conductivity, reflectivity, extinction coefficient, absorption coefficient, and electron energy loss function (EELF), all evaluated as functions of photon energy.

6.1 Dielectric Function

The interaction of electromagnetic radiation with a material is described by the complex dielectric function, given by:

$$\varepsilon(\omega) = \varepsilon_1(\omega) + i\varepsilon_2(\omega)$$

where $\varepsilon_1(\omega)$ represents the real part associated with polarization and dispersion, and denotes the imaginary part corresponding to optical absorption and energy dissipation [29]. The optical spectra are primarily governed by interband electronic transitions.

The calculated imaginary part of the dielectric function exhibits a dominant peak in the infrared region (0.08–0.31 eV), followed by smaller peaks in the visible range (1.13–1.86 eV). At zero photon energy, the static dielectric constants are obtained as follows: Co_2CrAl: $\varepsilon_1(0)$ = 311.85, $\varepsilon_2(0)$ = 140.75; Co_2CrBi: $\varepsilon_1(0)$ = 300.15, $\varepsilon_2(0)$ = 112.10; Co_2CrGe: $\varepsilon_1(0)$ = 287.60, $\varepsilon_2(0)$ = 105.90 and Co_2CrSi: $\varepsilon_1(0)$ = 291.10, $\varepsilon_2(0)$ = 98.80.

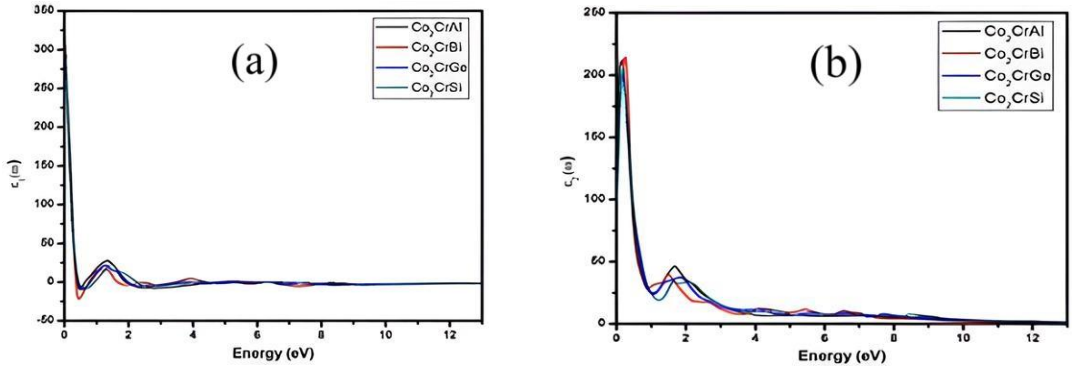

Fig. 4: Calculated optical parameters (a) real part of dielectric function (b) imaginary part of dielectric function for Co_2CrX (X = Al, Bi, Ge, Si).

6.2 Optical Conductivity

Optical conductivity provides insight into charge carrier dynamics under an applied electromagnetic field. The calculated spectra display prominent peaks in the energy range of 5.4-8.6 eV, with a notable feature between 1.6 and 2.3 eV. Additional peaks observed in the infrared region (0.18-0.50 eV and 1.38-1.88 eV) indicate strong interband electronic transitions.

6.3 Absorption Coefficient

The absorption coefficient increases with photon energy, spanning the visible to ultraviolet regions. Maximum absorption peaks are observed between 7.50 and 8.75 eV for all compounds, indicating strong photon absorption in this energy range and suggesting their suitability for ultraviolet optoelectronic applications.

Journal of Information Systems Engineering and Management
2024, 9(4)
e-ISSN: 2468-4376
https://www.jisem-journal.com/

Research Article

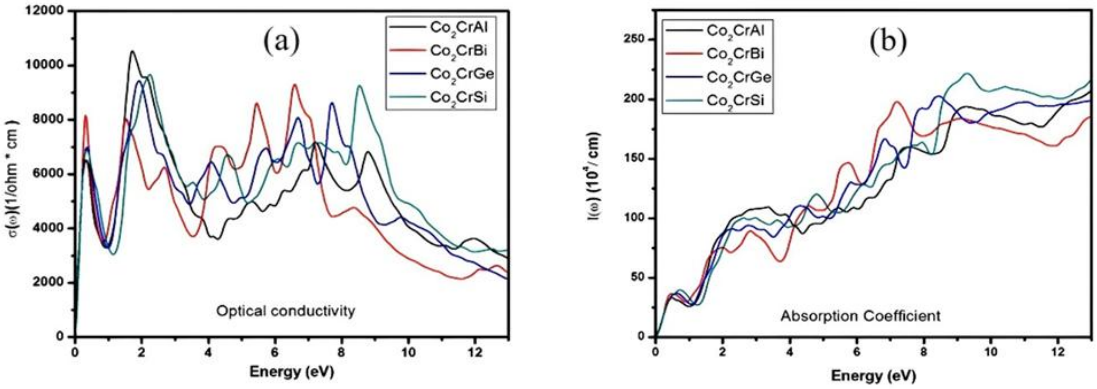

Fig. 5: Calculated optical parameters (a) optical conductivity (b) absorption coefficient for Co_2CrX (X = Al, Bi, Ge, Si).

6.4 Electron Energy Loss Function

The electron energy loss function (EELF) characterizes the energy loss of fast electrons traversing the material. A pronounced peak corresponding to the plasma frequency marks the transition from metallic to dielectric behavior. Below this frequency, the material exhibits metallic characteristics, whereas dielectric behavior dominates above it. The EELF increases from the infrared to ultraviolet region, with maximum energy loss occurring between 12 and 13 eV.

6.5 Extinction Coefficient

The extinction coefficient spectrum shows a strong peak in the infrared region (0.12–0.54 eV), followed by a gradual decrease. A secondary peak appears in the visible region (1.16–2.59 eV), along with a weaker feature near 8 eV in the ultraviolet range.

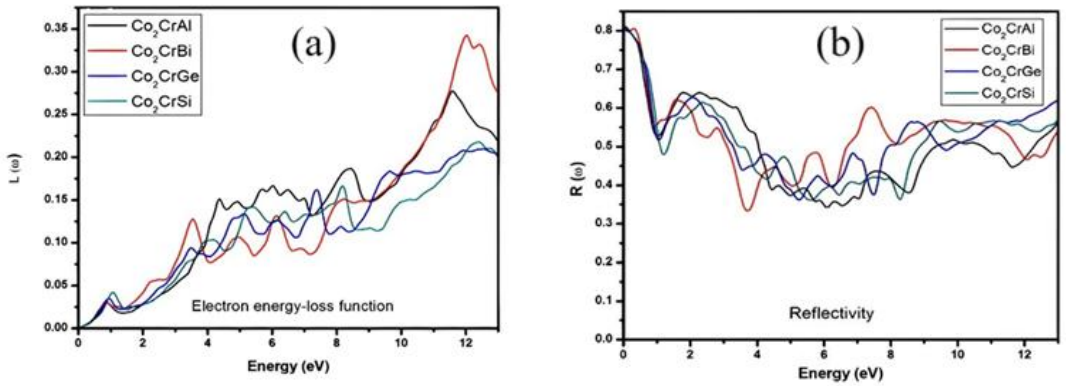

Fig. 6: Calculated optical parameters (a) electron energy-loss function (b) reflectivity for Co_2CrX (X = Al, Bi, Ge, Si).

6.6 Reflectivity

Reflectivity determines the fraction of incident electromagnetic radiation reflected from the material surface. The static reflectivity values are calculated as: Co_2CrAl (0.808), Co_2CrBi (0.804), Co_2CrGe (0.800), and Co_2CrSi (0.796). Reflectivity initially decreases with increasing photon energy, reaching a minimum near 2 eV, and subsequently increases toward the ultraviolet region (~8.3 eV). This trend is inversely related to the absorption coefficient and is consistent with typical optical behavior.

6.7 Refractive Index

The refractive index is a key optical parameter governing light propagation, dispersion, and total internal reflection. At zero frequency, the calculated refractive indices are: Co_2CrAl (18.09), Co_2CrBi (17.63), Co_2CrGe (17.28), and Co_2CrSi (17.26). These high values indicate strong light–matter interaction and significant dispersion potential in these compounds.

Journal of Information Systems Engineering and Management
2024, 9(4)
e-ISSN: 2468-4376
https://www.jisem-journal.com/

Research Article

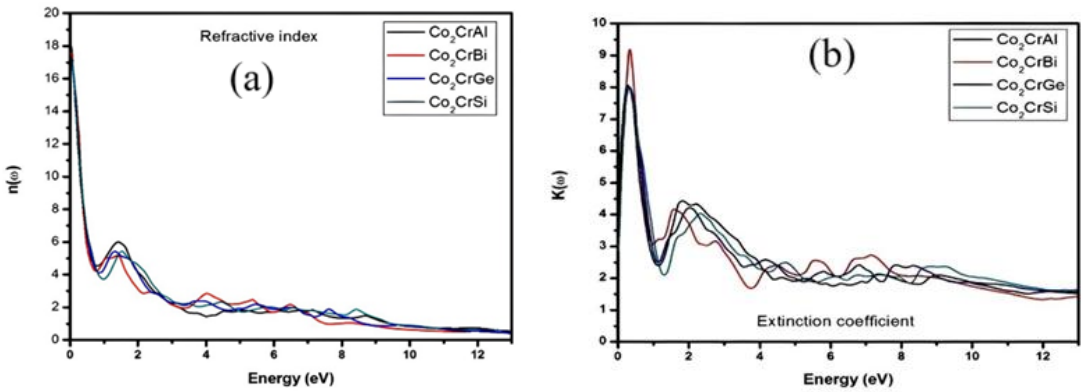

Fig. 7: Calculated optical parameters (a) refractive index and (b) extinction coefficient for Co_2CrX (X = Al, Bi, Ge, Si).

7. Conclusions

In this study, a comprehensive first-principles investigation of the structural, electronic, magnetic, elastic, and optical properties of Co2CrX (X = Al, Bi, Ge, Si) full-Heusler compounds has been carried out using the FP-LAPW method within the WIEN2k framework, employing the generalized gradient approximation (GGA) for exchange–correlation effects.

The electronic structure analysis, based on band structure and density of states calculations, confirms that all studied compounds exhibit half-metallic behavior with 100% spin polarization. The compounds crystallize in the cubic L21 structure and are found to be energetically stable. The calculated magnetic moments follow the Slater–Pauling rule, demonstrating excellent agreement with theoretical predictions.

The optical properties, including dielectric function, optical conductivity, reflectivity, refractive index, absorption coefficient, extinction coefficient, and electron energy loss function, have been systematically analyzed over a wide photon energy range. The results indicate strong interband transitions, high optical absorption, and significant dispersion characteristics.

Overall, the Co_2CrX (X = Al, Bi, Ge, Si) compounds exhibit a unique combination of half-metallicity, robust ferromagnetism, and favorable optical properties, making them promising candidates for future spintronic and optoelectronic applications.

References

[1] Heusler, F. (1903). Über magnetische Manganlegierungen. Verhandlungen der Deutschen Physikalischen Gesellschaft, 5, 219–223.

[2] Bradley, A. J., & Rogers, J. W. (1934). The crystal structure of Heusler alloys. Proceedings of the Royal Society A: Mathematical, Physical and Engineering Sciences, 144(852), 340–359. https://doi.org/10.1098/rspa.1934.0034

[3] de Groot, R. A., Mueller, F. M., van Engen, P. G., & Buschow, K. H. J. (1983). New class of materials: Half-metallic ferromagnets. Physical Review Letters, 50(25), 2024–2027. https://doi.org/10.1103/PhysRevLett.50.2024

[4] Wollmann, L., Nayak, A. K., Parkin, S. S. P., & Felser, C. (2017). Heusler 4.0: Tunable materials. Annual Review of Materials Research, 47, 247–270. https://doi.org/10.1146/annurev-matsci-070616-123928

[5] Tavares, S., Costa, M., Lima, M. S., & Araújo, J. P. (2023). Spintronic properties of full and half Heusler compounds: A review. Progress in Materials Science, 132, 101017. https://doi.org/10.1016/j.pmatsci.2022.101017

Research Article

[6] Bai, Z., Shen, L., Han, G., & Feng, Y. P. (2013). A review on Heusler compounds for spintronic applications. arXiv preprint, arXiv:1304.1747. https://arxiv.org/abs/1304.1747
[7] Meyers, F., Wolff, M., & Felser, C. (2023). Recent developments in Heusler materials for magnetic and electronic applications. APL Materials, 11(1), 010701. https://doi.org/10.1063/5.0128930
[8] Blaha, P., Schwarz, K., Madsen, G. K., Kvasnicka, D., & Luitz, J. (2001). wien2k. An augmented plane wave+ local orbitals program for calculating crystal properties, 60(1), 155-169.
[9] Sjöstedt, E., Nordström, L., & Singh, D. J. (2000). An alternative way of linearizing the augmented plane-wave method. Solid State Communications, 114(1), 15-20. https://doi.org/10.1016/S0038-1098(99)00577-3
[10] Perdew, J. P., Burke, K., & Ernzerhof, M. (1996). Generalized gradient approximation made simple. Physical review letters, 77(18), 3865. https://doi.org/10.1103/PhysRevLett.77.3865
[11] Monkhorst, H. J., & Pack, J. D. (1976). Special points for Brillouin-zone integrations. Physical review B, 13(12), 5188. https://doi.org/10.1103/PhysRevB.13.5188
[12] Wollmann, L., Nayak, A. K., Parkin, S. S. P., & Felser, C. (2017). Heusler 4.0: Tunable materials. Annual Review of Materials Research, 47, 247–270. https://doi.org/10.1146/annurev-matsci-070616-123928
[13] Graf, T., Felser, C., & Parkin, S. S. P. (2011). Simple rules for the understanding of Heusler compounds. Progress in Solid State Chemistry, 39(1), 1–50. https://doi.org/10.1016/j.progsolidstchem.2011.02.001
[14] Murnaghan, F. D. (1944). The compressibility of media under extreme pressures. Proceedings of the National Academy of Sciences, 30(9), 244–247. https://doi.org/10.1073/pnas.30.9.244
[15] Webster, P. J. (1971). Magnetic and chemical order in Heusler alloys containing cobalt and manganese. Journal of Physics and Chemistry of Solids, 32(6), 1221–1231. https://doi.org/10.1016/S0022-3697(71)80161-1
[16] Galanakis, I., Dederichs, P. H., & Papanikolaou, N. (2002). Origin and properties of the gap in the half-ferromagnetic Heusler alloys. Physical Review B, 66(17), 174429. https://doi.org/10.1103/PhysRevB.66.174429
[17] Block, T., et al. (2003). Epitaxial growth and magnetic properties of $Co_2Cr_{0.6}Fe_{0.4}Al$ thin films. Journal of Applied Physics, 93(5), 2871–2875. https://doi.org/10.1063/1.1542755
[18] Wurmehl, S., et al. (2005). Geometric, electronic, and magnetic structure of Co_2CrZ (Z = Si, Ge, Sn) investigated by X-ray diffraction, magnetometry, and Mössbauer spectroscopy. Journal of Physics: Condensed Matter, 17(12), 1877–1891. https://doi.org/10.1088/0953-8984/17/12/005
[19] Gao, G. Y., et al. (2008). Half-metallic ferromagnetism and origin of the minority-spin gap in Co_2CrZ (Z = Al, Ga, In, Si, Ge, Sn) Heusler compounds. Journal of Physics: Condensed Matter, 20(13), 135227. https://doi.org/10.1088/0953-8984/20/13/135227
[20] Birsan, A., et al. (2013). First-principles calculations of electronic and magnetic properties of full-Heusler alloys Co_2CrZ (Z = Si, Ge, Sn). Journal of Magnetism and Magnetic Materials, 343, 92–96. https://doi.org/10.1016/j.jmmm.2013.04.021
[21] Sukhender, S., Mohan, L., Kumar, S., Bhardwaj, S. R., & Verma, A. S. (2020). Electronic, Optical, Elastic and Magnetic Properties of Co_2VZ (Z= As, B, In, Sb) Full Heusler Compounds. East European Journal of Physics, (4), 51-62. https://doi.org/10.26565/2312-4334-2020-4-07
[22] Gökog, G. (2010). First principles electronic structure calculations of Co_2CrBi Heusler system. Physica B: Condensed Matter, 405(9), 2162-2165. https://doi.org/10.1016/j.physb.2010.01.126
[23] Yahya, S. J., Abu-Jafar, M. S., Al Azar, S., Mousa, A. A., Khenata, R., Abu-Baker, D., & Farout, M. (2022). The structural, electronic, magnetic and elastic properties of full-Heusler Co_2CrAl and Cr_2MnSb: An ab initio study. Crystals, 12(11), 1580. https://doi.org/10.3390/cryst12111580

Research Article

[24] Rai, D. P., et al. (2011). Study of energy bands and magnetic properties of Co2CrSi Heusler alloy. Bulletin of Materials Science, 34(6), 1219–1222. https://doi.org/10.1007/s12034-011-0233-y
[25] Rai, D. P., Shankar, A., Sandeep, Ghimire, M. P., & Thapa, R. K. (2013). Electronic and magnetic properties of a full-Heusler alloy Co 2 CrGe: a first-principles study. Journal of Theoretical and Applied Physics, 7, 1-6. https://doi.org/10.1186/2251-7235-7-3
[26] Aly, S. H., & Shabara, R. M. (2014). First principles calculation of elastic and magnetic properties of Cr-based full-Heusler alloys. Journal of magnetism and magnetic materials, 360, 143-147. https://doi.org/10.1016/j.jmmm.2014.02.030
[27] Galanakis, I., Dederichs, P. H., & Papanikolaou, N. J. P. R. B. (2002). Origin and properties of the gap in the half-ferromagnetic Heusler alloys. Physical Review B, 66(13), 134428. https://doi.org/10.1103/PhysRevB.66.134428
[28] J. C. Slater, The Ferromagnetism of Nickel, Phys. Rev. 49 (1936) 537-545. https://doi.org/10.1103/PhysRev.49.537
[29] Pauling, L. (1938). The nature of the interatomic forces in metals. Physical Review, 54(11), 899. https://doi.org/10.1103/PhysRev.54.899
[30] Yu, P. Y., & Cardona, M. (2010). Fundamentals of Semiconductors: Physics and Materials Properties (4th ed.). Springer.